

## Accepted Manuscript

Title: Pulsed direct current magnetron sputtered nanocrystalline tin oxide films

Authors: A. Sivasankar, N.M. Figueiredo, A. Cavaleiro

PII: S0169-4332(12)00971-3  
DOI: doi:10.1016/j.apsusc.2012.05.112  
Reference: APSUSC 23738

To appear in: *APSUSC*

Received date: 24-8-2011  
Revised date: 5-4-2012  
Accepted date: 22-5-2012



Please cite this article as: A. Sivasankar, A. Cavaleiro, Pulsed direct current magnetron sputtered nanocrystalline tin oxide films, *Applied Surface Science* (2010), doi:10.1016/j.apsusc.2012.05.112

This is a PDF file of an unedited manuscript that has been accepted for publication. As a service to our customers we are providing this early version of the manuscript. The manuscript will undergo copyediting, typesetting, and review of the resulting proof before it is published in its final form. Please note that during the production process errors may be discovered which could affect the content, and all legal disclaimers that apply to the journal pertain.

# Pulsed direct current magnetron sputtered nanocrystalline tin oxide films

A. Sivasankar Reddy, N.M. Figueiredo, A. Cavaleiro\*  
SEG-CEMUC- Department of Mechanical Engineering, University of Coimbra, 3030-788  
Coimbra, Portugal

## Abstract

The nanocrystalline tin oxide ( $\text{SnO}_2$ ) films were deposited on glass substrates by pulsed magnetron sputtering technique and subsequently annealed from 200 to 500 °C. The structural, microstructural, electrical, and optical properties of as deposited and annealed  $\text{SnO}_2$  films were studied. The crystallinity degree of the films increased with annealing temperature. Photoluminescence (PL) measurements showed that the emission peaks have low intensity and are positioned at 535 nm (2.31 eV) and 605 nm (2.05 eV) in as deposited  $\text{SnO}_2$  films. The intensity of PL peak increases sharply with the increasing of annealing temperature. The as deposited films exhibited high electrical resistivity and low optical transmittance. After annealing at 500 °C, the electrical resistivity of the films decreased to the lowest value of 0.015  $\Omega\text{cm}$ , being the optical transmittance 90%.

*Keywords:* A. Oxides, B. Thin films, C. Sputtering, D. Electrical, E. Optical.

-----  
\*Corresponding author.

Tel: + 351 239 790745, Fax: +351 239 790701

*E-mail address:* [albano.cavaleiro@dem.uc.pt](mailto:albano.cavaleiro@dem.uc.pt) (A. Cavaleiro)

[akepati77@gmail.com](mailto:akepati77@gmail.com) (A.S. Reddy)

## 1. Introduction

Tin oxide ( $\text{SnO}_2$ ) thin films are attractive in a wide range of applications, e.g., gas sensors, transparent electrodes, heat mirrors, solar cells, thin film resistors, antireflection coatings [1,2], due to their unique properties of high optical transparency in the visible region with low electrical resistivity. Additionally,  $\text{SnO}_2$  films are chemically and thermally stable, and mechanically harder than  $\text{ZnO}$  films [3]. In the past few years, nanocrystalline  $\text{SnO}_2$  has been reported to have some different characteristics from the bulk crystals, and much attention has been focused on the synthesis and investigation of the novel properties of  $\text{SnO}_2$  nanowires, nanorods, nanobelts, and nanotubes [4]. Various thin film deposition techniques including sputtering [5], laser-assisted chemical vapor deposition [6], pulsed laser evaporation [7], electrodeposition [8], and metalorganic chemical vapor deposition [9] have been used to deposit  $\text{SnO}_2$  films. Among these techniques, pulsed magnetron sputtering has recently become a very popular method of thin film deposition, due to its versatility, high stability, controllability, repeatability, low environmental impact and ability to provide uniform coatings over large area substrates up to 4 m in width [10,11]. In this paper,  $\text{SnO}_2$  films were deposited on unheated glass substrates by pulsed magnetron sputtering from a pure Sn target in the presence of oxygen and subsequently annealed in air at different temperatures. The structural, microstructural, electrical and optical properties of as deposited and annealed films were investigated.

## 2. Experimental

The  $\text{SnO}_2$  films were deposited on cleaned glass substrates by pulsed magnetron sputtering using a Sn target (15cmx15cmx0.7cm, 99.99% purity). The deposition was carried out in a reactive atmosphere in the presence of a mixture of pure Ar and  $\text{O}_2$  gases, with a molar ratio Ar: $\text{O}_2$  of 0.5. The deposition pressure was fixed at approximately 0.7 Pa. The substrate holder

was neither biased nor intentionally heated and it was set to a constant rotation speed of 20 r.p.m.. The target to substrate distance was fixed at 6 cm. Before deposition, an ultimate vacuum pressure better than  $7 \times 10^{-4}$  Pa was reached. The substrates surface was ion cleaned with an ion gun. The cleaning procedure included first an electron heating and afterwards an Ar<sup>+</sup> bombardment, for 10 minutes each (ion gun settings at 20A, 40V and substrate bias progressively increased to -70V). During the deposition of the films, the power on the target was fixed at 900W. The as deposited films were post-annealed at 200, 300 and 500 °C in air. The films thickness was approximately ~200 nm. The chemical composition of the coatings was determined by an electron probe microanalysis (EPMA) apparatus equipped with wavelength-dispersive X-ray spectroscopy (WDX). The structural properties of the films were determined by X-ray diffraction (XRD). The surface morphology and microstructure was characterized by atomic force microscopy (AFM), and scanning electron microscopy (SEM), respectively. The photoluminescence (PL) spectra were measured with a LS55 fluorescence spectrometer (Perkin Elmer) at room temperature. The electrical properties of the films were measured by four point probe technique and the optical transmittance was recorded using a UV-Vis-NIR double beam spectrophotometer.

### 3. Results and discussion

The chemical composition of as deposited and annealed (500 °C) SnO<sub>2</sub> films is listed in Table 1. EPMA results show that the SnO<sub>2</sub> films contain tin and oxygen. The Sn/O ratio is close to the stoichiometric compound of SnO<sub>2</sub> after annealing the films at 500 °C.

Sample history	Atomic percentage		
	Sn	O	Sn/O
As deposited	36.2	63.8	0.57
500 °C	34.3	65.7	0.52

**Table 1.** Chemical composition of pulsed dc magnetron sputtered SnO<sub>2</sub> films .

### 3.1. Film structure and surface morphology

Fig.1 shows XRD patterns of the as deposited and annealed SnO<sub>2</sub> films. From the results, neither Sn nor sub-stoichiometry SnO<sub>2</sub> phases were found in the as deposited and annealed films. The as deposited and annealed films were polycrystalline with tetragonal structure. The as deposited films exhibited broad peaks corresponding to the (110), (200), and (211) reflections. With the annealing temperature, the peaks became progressively narrower and new reflections appeared, (101) at 200°C and (220) at 500 °C. The presence of broad peaks indicates that SnO<sub>2</sub> has very small crystallite sizes [12] which increase with annealing temperature. With this trend, the diffraction peaks were shifted to increasing higher angles. The lattice parameters  $a$  and  $c$  for the tetragonal structure were calculated from the equation,

$$\frac{1}{d_{hkl}^2} = \frac{h^2 + k^2}{a^2} + \frac{l^2}{c^2}$$

where  $d_{hkl}$  is interplanar spacing,  $h$ ,  $k$ , and  $l$  are all integer indexes of the lattice plane, and  $a$  and  $c$  are lattice constants [13].

The lattice parameters  $a$  and  $c$ , calculated from the (110) and (211) peaks, are listed in Table 2. It is observed that with increasing annealing temperature the lattice parameter  $a$  decreases whereas  $c$  increases. Chen et al. [4] suggested that in the as deposited films a large number of oxygen vacancies, vacancy clusters, and local lattice disorder can occur, which lead to an increase in  $a$  and a decrease in  $c$ . With the annealing temperature, a progressive removing of the oxygen vacancies and lattice defects takes place with the consequent decrease in  $a$  and increase in  $c$  parameters, tending towards the equilibrium  $c/a$  ratio.

The grain size of the films was calculated from the Scherer's equation, neglecting the peak broadening due to residual stresses in the films,  $L = 0.9\lambda/(\beta\cos\theta)$ , where  $L$  is the grain size,

$\beta$  is full width at half maximum in radians, and  $\lambda$  is the wavelength of X-rays(1.7903Å). The as deposited film has average grain size of 4.1nm which progressively increased, after annealing at 200, 300, and 500 °C to 4.6nm, 5.4nm, and 7.3nm respectively.

Annealing Temperature (°C)	Lattice parameter (Å)	
	a	c
As deposited	4.762	3.155
200	4.756	3.174
300	4.733	3.179
500	4.722	3.193
ICDD (#88-0287)	4.737	3.186

**Table 2** Lattice parameters of as deposited and annealed SnO<sub>2</sub> films.

Scanning electron microscopy micrograph of the 500 °C annealed SnO<sub>2</sub> film is shown in Fig.2(a). A very smooth and compact surface is observed without any particular feature detected. Within the resolution of the SEM used apparatus, no cracks and voids could be detected. Fig.2(b) shows the atomic force microscopy image of the SnO<sub>2</sub> film annealed at 500 °C. It is seen that the film has a homogeneous and smooth surface, with a narrow distribution of small grains. The average RMS roughness of films was found to be 1.1 nm. From the histogram, we observed that the average grain size was ~5nm.

### 3.2. Photoluminescence properties

The room temperature PL spectra of the as deposited and 500 °C annealed SnO<sub>2</sub> nanocrystalline films are shown in Fig.3. The emission peaks have low intensity and are positioned at 535 nm (2.31 eV) and 605nm (2.05 eV) in as deposited SnO<sub>2</sub> films. After annealing the films at 500 °C, the dominant peak was slightly red shifted to 538nm and the intensity of the peaks sharply increased, especially the higher energy one. Transparent conducting oxides like

$\text{SnO}_2$  are n-type because of the existence of intrinsic defects, such as oxygen vacancies and/or metal interstitials [14]. In poly- and nano-crystalline oxides, oxygen vacancies are the most common defects and usually act as radiative centers in luminescence processes [15].

The observed PL red shift can be attributed to a combined effect of larger crystallite size and compressive stress [14], in good agreement with the present structural and microstructural results. The residual compressive stresses are arising during cooling down from annealing temperature and they are due to the mismatch between the coefficients of thermal expansion of the film ( $\text{SnO}_2$ ) and the substrate (glass). If the chemical composition of the as grown sample is taken into account, a very high number of oxygen vacancies should be present (O is sub-stoichiometric in relation to  $\text{SnO}_2$ ), much more than in the annealed case. Therefore, in principle stronger PL emission would be expected for the as grown sample. However, the presence of an excessive amount of defects can lead to additional competitive non-radiative recombination paths, which weakens the transition between the donor and the acceptor levels [14]. As the number of excessive defects in the film diminishes with thermal annealing, the non-radiative recombination processes also diminishes. In this way the PL intensity can in fact increase for the sample annealed at  $500^\circ\text{C}$ . On the other hand, the very low cooling rates used after the annealing process can affect the distribution of space charges in the nanoparticles with a vacancy migration from the bulk to the surface of the grains [16]. Therefore, despite the bigger and more ordered grains (with less “bulk” defects), more defective grain boundaries can be expected. In a study of the defects in  $\text{SnO}_2$  nanostructures made by Prades et al. [17] experimental bands were related to recombinations from conduction band and bulk shallow levels (mainly created by ionized bulk oxygen vacancies) to levels near the top of the valence band corresponding to surface oxygen vacancies. The  $100^\circ$  tin coordinated oxygen surface vacancy was related to two bands below 2.2

eV, whereas the 130° tin coordinated oxygen surface vacancy was related to two bands above 2.37 eV. Analogously in the present case, the two different emissions can arise from recombinations involving surface oxygen vacancies with different tin coordination. The lower energy band located at ~605 nm should correspond to recombination involving the 100° tin coordinated oxygen surface vacancy; the higher energy band located around ~535 nm should correspond to recombination involving the 130° tin coordinated oxygen surface vacancy. Since the 130° coordination vacancies require more thermal energy than the 100° coordinated ones [17] they should appear more pronouncedly with increasing temperature, fact that is observed in this study for 500°C.

Zhu et al.[18] reported broad PL bands centered at around 530 nm and 605 nm for SnO<sub>2</sub> films grown at 500 and 700 °C, respectively. Hu et al.[19] observed a strong emission band at ~605 nm in SnO<sub>2</sub> ribbons. A broad luminescence peak at 615 nm was reported by Luan et al.[20] in metalorganic chemical vapor deposition SnO<sub>2</sub> films prepared at 600 °C.

### 3.3. *Electrical properties*

In general, the thermal treatment of the thin films is applied to enhance the properties of the as deposited films. The variation of the electrical resistivity of SnO<sub>2</sub> films as function of annealing temperature is shown in Fig.4. The as deposited film shows an electrical resistivity of 0.76Ωcm, which decreases progressively down to 0.015Ωcm with increasing annealing temperature up to 500 °C. The decrease in resistivity is mainly attributed to the improvement of the crystallinity of the films at higher temperature either by grain growing or lattice defects annihilation which reduces the number of scattering centers. The cooling rate is found to have influence on film resistance as well as on the reduction of gases [16] and, thus, the slow cooling rates used in this study should contribute for the improvement of the structure and a decrease of lattice defects.



### 3.4. Optical properties

Fig. 5 shows the optical transmittance spectra in the wavelength range 250–1000 nm for SnO<sub>2</sub> films at various annealing temperatures. With annealing temperature, both a shift in the absorption edge towards shorter wavelengths and an increase in the average transmission were observed. The maximum in the optical transmittance of the films in the visible region was improved from 79% for the as deposited films to 90 % when the films was annealed at 500 °C. The increase of transmittance with annealing temperature may be due to the decreasing optical scattering caused by the densification of grains followed by the grain growth [21]. When the annealing temperature increases, the stoichiometry of the thin films is improved, i.e. defect number decreases. The optical properties of films was also found to be influenced by the surface morphology, the smoother film with less grain boundaries has the higher transmittance [22]. The increase in optical transmittance with temperature can be attributed to the increase of structural homogeneity and crystallinity [23].

The optical absorption coefficient ( $\alpha$ ) was evaluated from the optical transmittance (T) and reflectance (R) data using the relation,

$$T = (1-R)^2 \exp(-\alpha t)$$

where  $t$  is the film thickness. The optical band gap ( $E_g$ ) of the films was estimated from the intercept plot of  $(\alpha h\nu)^2$  versus photon energy ( $h\nu$ ) which assumes the direct transition between the top of the valance band and the bottom of the conduction band using the relation [24],

$$(\alpha h\nu) = A (h\nu - E_g)^{1/2}$$

where  $A$  is the absorption edge width parameter. Extrapolation of the linear portion of the plots of  $(\alpha h\nu)^2$  versus photon energy of  $\text{SnO}_2$  films to  $\alpha = 0$  results in the optical band gap of the films.

The  $(\alpha h\nu)^2$  versus photon energy ( $h\nu$ ) plot for as deposited and annealed  $\text{SnO}_2$  films is presented in Fig.6. The as deposited film exhibited the optical band gap of 3.79 eV, and after thermal annealing the band gap increased from 3.85 to 3.93 eV with increasing temperature from 200 to 500 °C. The results in the literature vary depending on the deposition and posterior annealing treatment. A similar behavior was reported by Kim et al.[25], for rf sputtered  $\text{SnO}_{2-x}$  films. Khan et al. [26] observed the drastic improvement of the band gap in electron beam evaporated nanocrystalline  $\text{SnO}_2$  films. The band gap increased from 3.61 to 4.22 eV, from as deposited film to 550 °C annealed one. However, Yadav et al. [27], achieved a much lower optical band gap of 3.28 eV with optical transmittance of 85 % in chemical reactive evaporated  $\text{SnO}_2$  films. On the other hand, Cetinorgu et al. [28], reported very high optical band gap of 4.35 eV with an average visible transmittance of 90 %, when the annealing temperature was 600 °C. Unfortunately, due to the type of substrate used in this work, it was not possible to reach this highest temperature. The increases of the optical band gap should be due to the improvement in the film structure; the decrease in the lattice defects with the improvement of crystallinity gives rise to a less amount of band gap defects with the consequent enlargement of the band gap energy. The optical performance of the  $\text{SnO}_2$  films achieved in this investigation, with an optical transmittance of 90% and an optical band gap of 3.93 eV after annealing at 500 °C, seems to be promising, particularly if higher temperatures can be tested. The obtained optical transmittance and band gap of  $\text{SnO}_2$  films are listed in Table 3.

Annealing temperature (°C)	Transmittance at 565 nm (%)	Band gap (eV)
As deposited	79	3.79
200	83	3.85
300	86	3.88
500	90	3.93

**Table 3** Optical transmittance and band gap of as deposited and annealed SnO<sub>2</sub> films.

### 3.5. Figure of Merit

The quality of a transparent conducting oxide can be judged by the parameter of figure of merit. The figure of merit was determined from the optical transmittance and sheet resistance ( $R_s$ ) data by using Scropp formula [29],

$$F = -1 / (\rho \ln T)$$

Where T is the transmittance, and  $\rho$  is the electrical resistivity

Fig.7 shows the variation in the figure of merit of SnO<sub>2</sub> with annealing temperature. As it would be expected, the as deposited films shows the low figure of merit of  $5.6 \Omega^{-1} \text{cm}^{-1}$ . After annealing, the values sharply increased from  $3.9 \times 10^1$  to  $6.2 \times 10^2 \Omega^{-1} \text{cm}^{-1}$  with the increase of annealing temperature from 200 to 500 °C. The highest figure of merit of  $6.2 \times 10^2 \Omega^{-1} \text{cm}^{-1}$  achieved after thermal annealing at 500 °C is due to the low electrical resistivity and high optical transmittance that were achieved.

## 4. Conclusion

Nanocrystalline SnO<sub>2</sub> films were deposited by pulsed magnetron sputtering on unheated glass substrates and posteriorly annealed at increasing temperatures up to 500 °C. The films were fairly uniform and had very smooth surface without cracks and voids. XRD results revealed an improvement of the crystallinity degree and an increase of the grain size with annealing

temperature. The electrical resistivity of the annealed films was almost two orders of magnitude lower than that of the as deposited films. A progressive improvement of the optical transmittance and band gap of the films was achieved with temperature. At 500 °C, the SnO<sub>2</sub> films showed the lowest electrical resistivity of 0.015 Ωcm, an optical transmittance of 90%, and high figure of merit of  $6.2 \times 10^2 \Omega^{-1} \text{cm}^{-1}$ , which makes it promising for optoelectronic devices.

### Acknowledgement

This research is partially sponsored by FEDER funds through the program COMPETE - Programa Operacional Factores de Competitividade - and by national funds through FCT - Fundação para a Ciência e a Tecnologia -, under the project DECOMAT: PTDC/CTM/70037/2006.

### References

- [1] M. Ichimura, K. Shibayama, K. Masui, *Thin Solid Films* 466 (2004) 34-36.
- [2] H.H. Afify, F.S. Terra, R.S. Momtaz, *J. Mater. Sci. Mater. Electron.* 7 (1996) 149-153.
- [3] E. Cetinorgu, C. Gumus, S. Goldsmith, F. Mansur, *Phys. Stat. sol. (a)* 204 (2007) 3278-3285.
- [4] Z.W. Chen, J.K.L. Lai, C.H. Shek, *Physical review B* 70 (2004) 1653141-653147.
- [5] Y.H. Choi, S.H. Hong, *Sensors and Actuators B* 125 (2007) 504-509.
- [6] M. Kwoka, L. Ottaviano, N. Waczynska, S. Santucci, J. Szuber, *Applied Surface Science* 256 (2010) 5771-5775.
- [7] R. Khandelwal, A.P. Singh, A. Kapoor, S. Grigorescu, P. Miglietta, N.E. Stankova, A. Perrone, *Optics & Laser Technology* 41 (2009) 89-93.
- [8] J. Yang, X. Li, S.L. Bai, R.X. Luo, A.F. Chen, Y. Lin, J.B. Zhang, *Thin Solid Films* 519 (2011) 6241-6245.
- [9] Z. Zhu, J. Ma, C. Luan, L. Kong, Q. Yu, *J. Luminescence* 131 (2011) 88-91.
- [10] J. O'Brien, P.J. Kelly, *Surface and Coatings Technology* 142-144 (2001) 621-627.
- [11] W.M. Posadowski, *Thin Solid Films* 343-344 (1999) 85-89.
- [12] F. Gu, S.F. Wang, M.K. Lu, G.J. Zhou, D. Xu, D.R. Yuan, *J. Phys. Chem. B* 108 (2004) 8119-8123.
- [13] *Thin films analysis by X-ray scattering*, Mario Birkholz, 2006 WILEY-VCH Verlag GmbH & Co. KGaA, Weinheim.
- [14] J. Ni, X. Zhao, X. Zheng, J. Zhao, B. Liu, *Acta Materialia* 57 (2009) 278-285.
- [15] F. Gu, S.F. Wang, C.F. Song, M.K. Lu, Y.X. Qi, G.J. Zhou, D. Xu, D.R. Yuan, *Chemical Physics Letters* 372 (2003) 451-454.
- [16] J. Liu, S. Gong, L. Quan, Z. Deng, H. Liu, D. Zhou, *Sensors and Actuators B* 145 (2010) 657-666.

- [17] J.D. Prades, J. Arbiol, A. Cirera, J.R. Morante, M. Avella, L. Zanotti, E. Comini, G. Faglia, G. Sberveglieri, *Sensors and Actuators B* 126 (2007) 6-12.
- [18] Z. Zhu, J. Ma, C. Luan, L. Kong, Q. Yu, *Journal of Luminescence* 131 (2011) 88–91.
- [19] J. Hu, Y. Bando, Q. Liu, D. Golberg, *Adv. Funct. Mater* 13 (2003) 493-496.
- [20] C. Luan, J. Ma, Z. Zhu, L. Kong, Q. Yu, *Journal of Crystal Growth* 318 (2011) 599–601.
- [21] H. Li, J. Wang, H. Liu, H. Zhang, X. Li, *J. Cryst.Growth* 275 (2005) e943-e946.
- [22] N. Bouhssira, S. Abed, E. Tomasella, J. Cellier, A. Mosbah, M.S. Aida, M. Jacquet, *Applied Surface Science* 252 (2006) 5594-5597.
- [23] I. Hambergend, C.G. Granquist, *J. Appl. Phys.* 60 (1986) R123-R159.
- [24] J. Tauc, *Amorphous and Liquid Semiconductors*, Plenum Press, New York, 1974.
- [25] I.H. Kim, J.H. Ko, D. Kim, K.S. Lee, T.S. Lee, J.-H. Jeong, B. Cheong, Y.-J. Baik, W.M. Kim, *Thin Solid Films* 515 (2006) 2475-2480.
- [26] A.F. Khan, M. Mehmooda, M. Aslam, M. Ashraf, *Applied Surface Science* 256 (2010) 2252–2258.
- [27] J.B. Yadav, R.B. Patil, R.K. Puri, V. Puri, *Mater. Sci. Eng. B* 139 (2007) 69-73.
- [28] E. Cetinorgu, S. Goldsmith, Y. Rosenbeerg, R.L. Boxman, *J. Non-Cryst. Solids* 353 (2007) 2595-2602.
- [29] F. merit: R.E.I. Scropp, C.E. Matovich, P.K. Bhatt, A.K. Madan, 20th IEEE, Photovoltaic Spec. Conf., Las Vegas, U.S.A., 1988.

Figure caption

Fig.1. XRD patterns of SnO<sub>2</sub> films as a function of annealing temperature.

Fig.2. SEM and AFM image of SnO<sub>2</sub> films annealed at 500 °C.

Fig.3. Room temperature PL spectra of SnO<sub>2</sub> films.

Fig.4. Electrical resistivity of SnO<sub>2</sub> films as a function of annealing temperature.

Fig.5. Optical transmittance spectra of SnO<sub>2</sub> films with different annealing temperatures.

Fig.6.  $(\alpha h\nu)^{1/2}$  versus the photon energy ( $h\nu$ ) for SnO<sub>2</sub> films with different annealing temperatures.

Fig.7. Figure of merit as a function of annealing temperature.

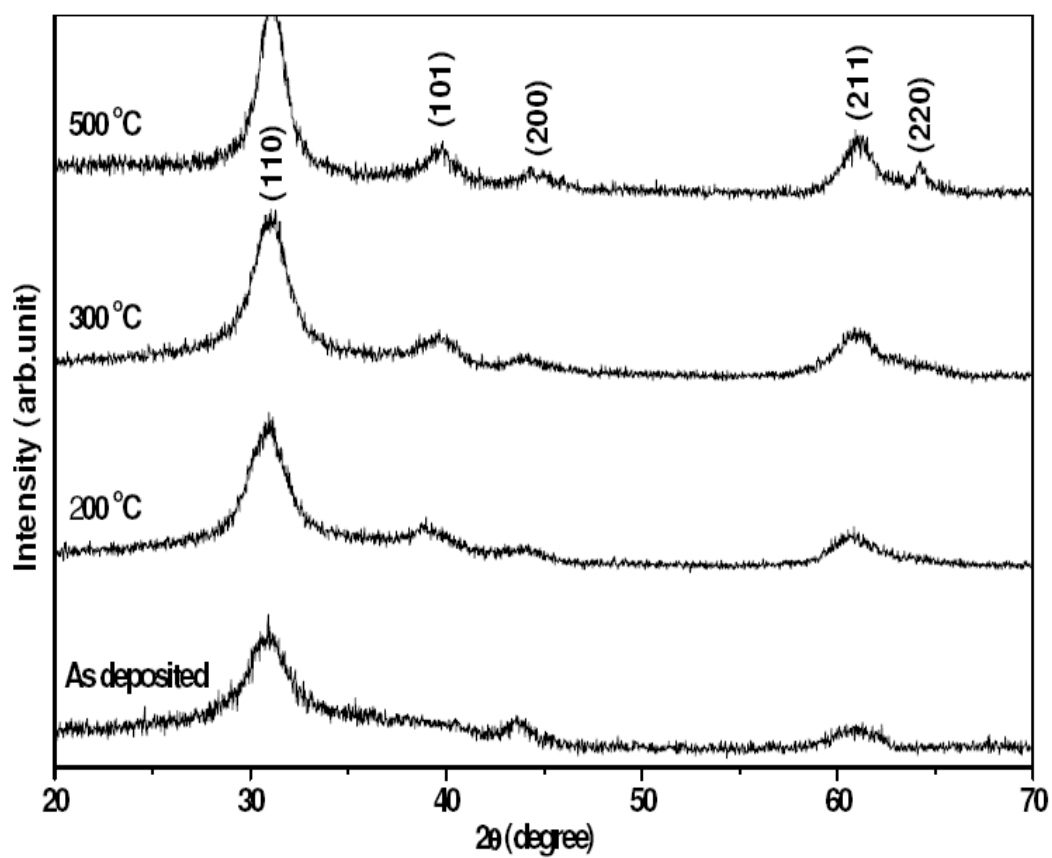
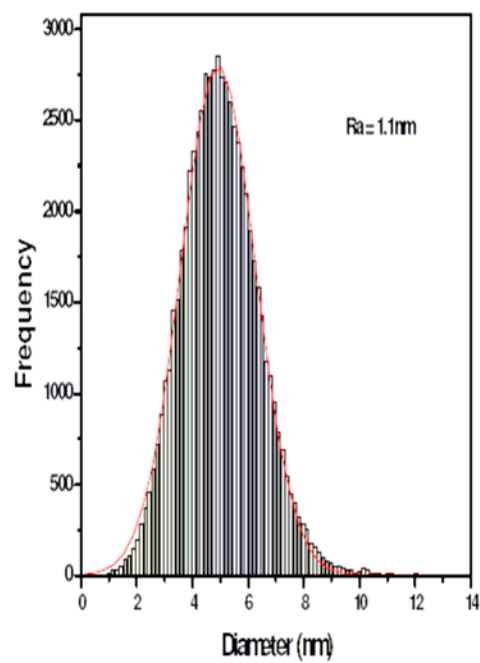
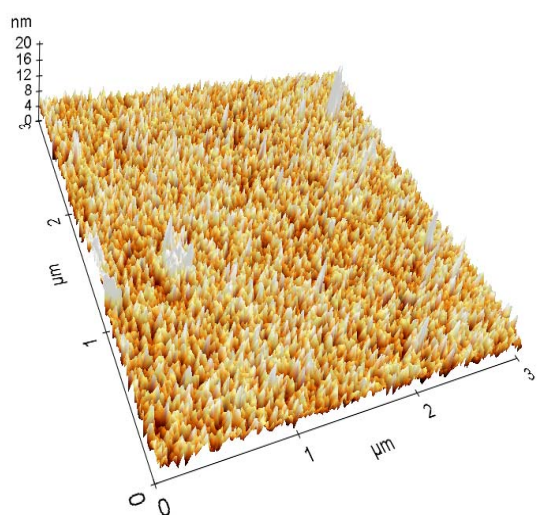
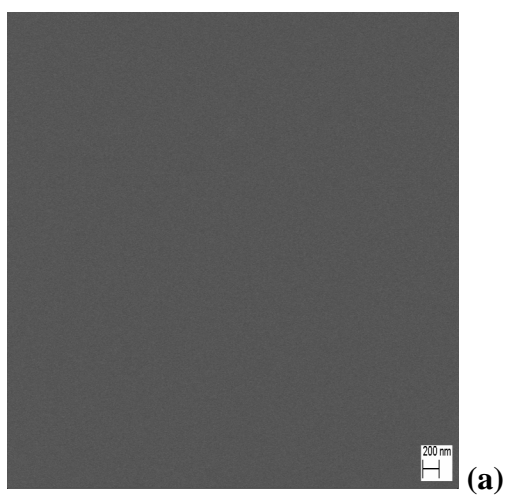


Figure 1



(b)

Figure 2



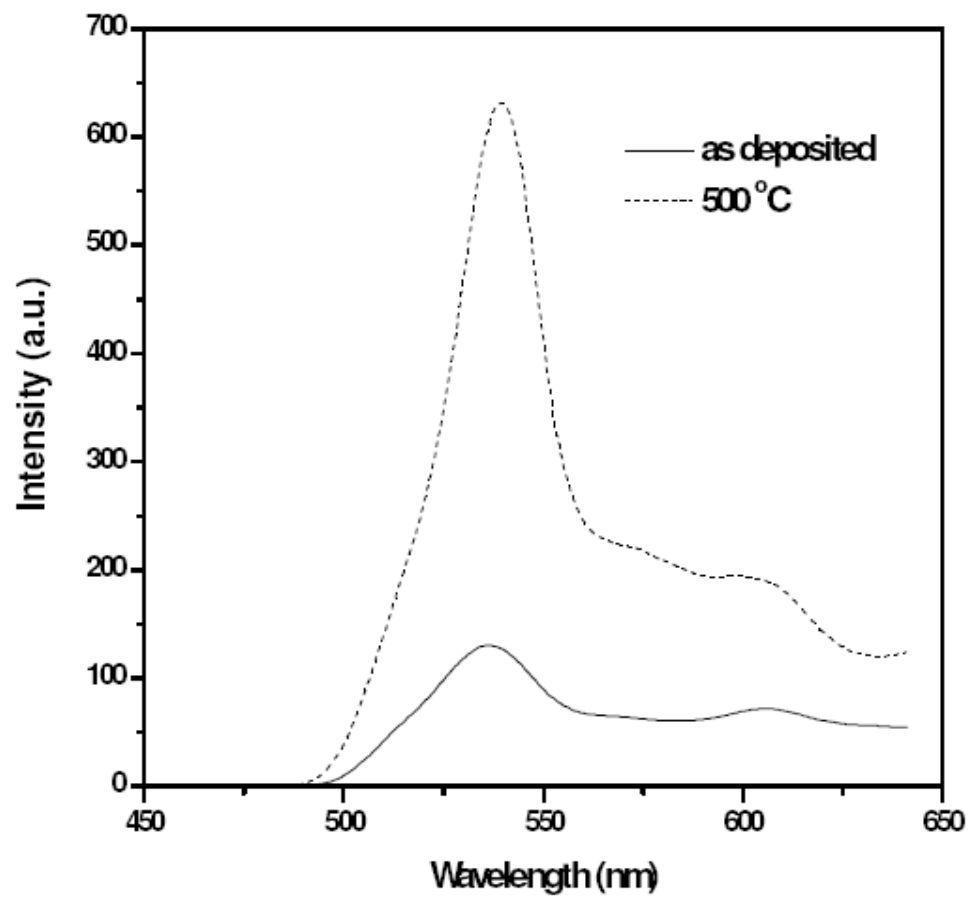
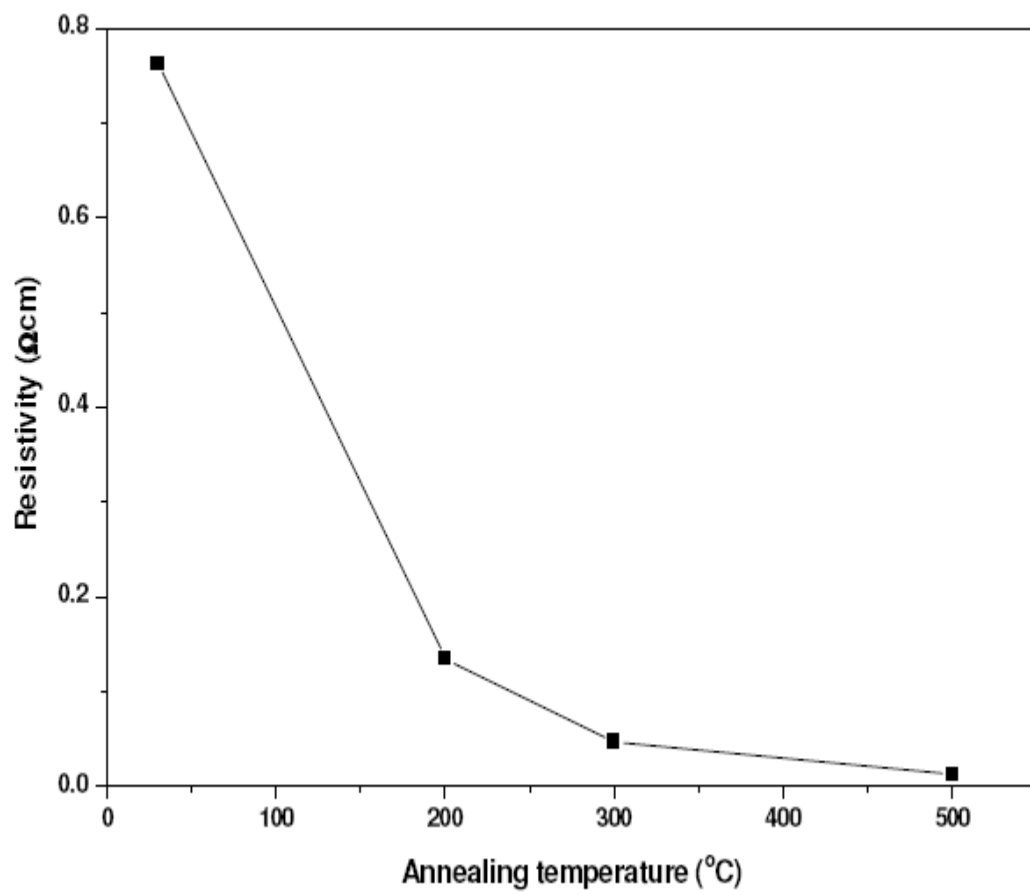


Figure 3

**Figure 4**

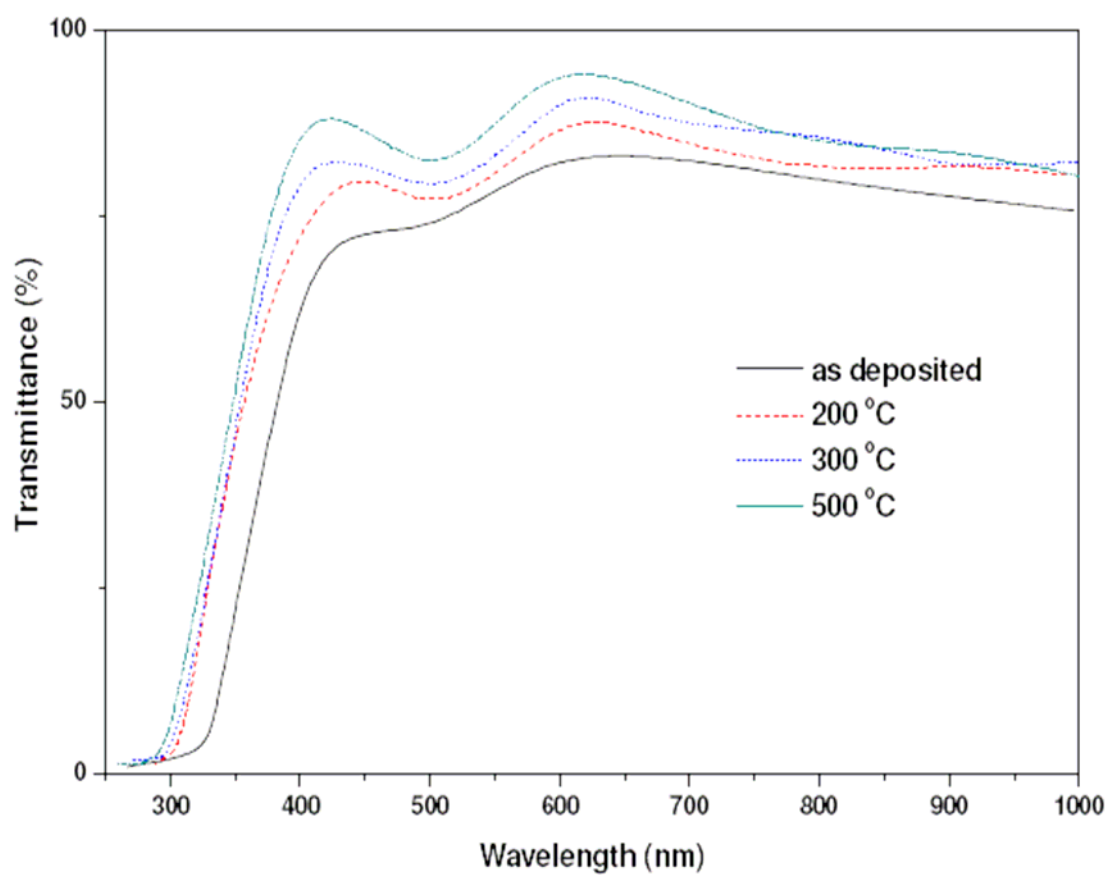


Figure 5

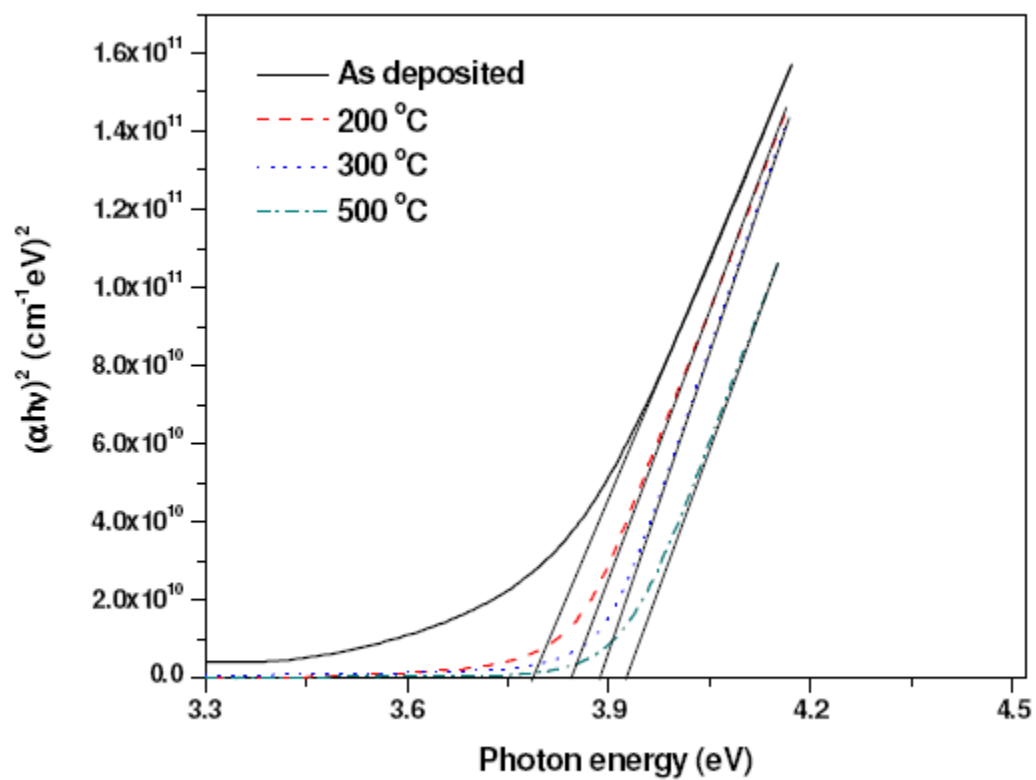
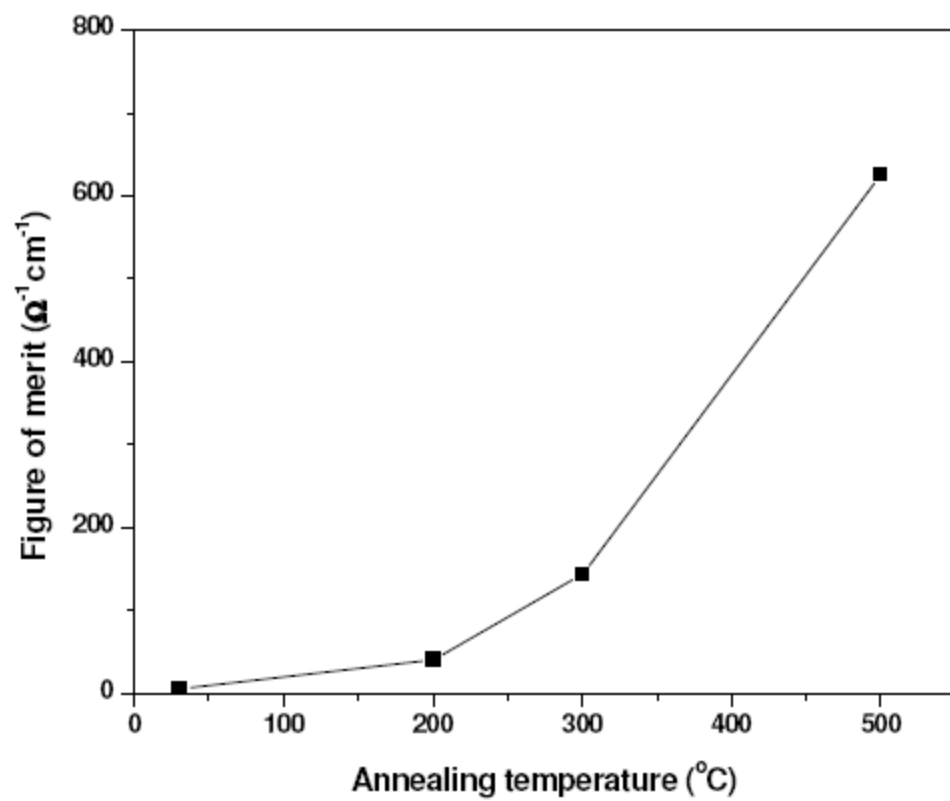


Figure 6

**Figure 7**

### Highlights

The nanocrystalline SnO<sub>2</sub> films were prepared by pulsed direct current magnetron sputtering

The crystallinity of the films was progressively improved by the annealing temperature

At the annealing temperature of 500 °C, the RMS roughness of the films was 1.1 nm

The red shift and improvement of the photoluminescence peaks intensity was found after annealed the films

The low electrical resistivity of 0.015 Ωcm with high optical transmittance of 90% were obtained at annealing temperature of 500 °C

Accepted Manuscript